


ULRR

Weak long-range diffusion

Item Type	Article
Authors	Garvey, Robert;Fowler, Andrew
Citation	Studies in Applied Mathematics, e12759
Publisher	Wiley Periodicals LLC
Download date	2026-04-17 21:33:31
Item License	https://creativecommons.org/licenses/by-nc-sa/4.0/
Link to Item	https://doi.org/10.34961/researchrepository-ul.26976784

Weak long-range diffusion

R. S. Garvey¹  | A. C. Fowler^{1,2}

¹MACSI, University of Limerick,
Limerick, Ireland

²OCIAM, University of Oxford, Oxford,
UK

Correspondence

R. S. Garvey, MACSI, University of
Limerick, Limerick, Ireland.
Email: Robert.Garvey@ul.ie

Funding information

Mathematics Applications Consortium
for Science and Industry; Science
Foundation Ireland, Grant/Award
Numbers: 12/IA/1683, 18/CRT/6049; SFI
Centre for Research Training in
Foundations of Data Science

Abstract

We study the spreading solutions of the nonlinear diffusion equation $c_t = [(\nu + c)c_x]_x$ when the far-field diffusivity ν is small. The method of strained coordinates is used to construct a uniform asymptotic correction to the similarity solution of the unperturbed problem. The equation provides a possible analogue to similar models of fluid jets and plumes.

KEYWORDS

jets, plumes, strained coordinates, weak long-range diffusion

1 | INTRODUCTION

The porous medium equation (e. g., Refs. 1–3) is a nonlinear diffusion equation given by

$$c_t = [cc_x]_x, \quad (1)$$

where c will generally represent the density or concentration of a certain substance, x and t represent space and time, and the subscripts indicate partial derivatives. Examples of its derivation arise in the consideration of the spread of a compressible fluid in a porous medium, where the variable c can represent either the fluid density or its pressure, and in saturated groundwater flow, where c would represent the elevation of the water table.

It is well known that a local release of the diffusing substance governed by (1) leads to its spread as a self-similarly evolving profile of compact support, bounded by fronts (where $c = 0$) that propagate outward at finite speed. Our interest here is in the case where the diffusivity c in (1) is modified

This is an open access article under the terms of the [Creative Commons Attribution](https://creativecommons.org/licenses/by/4.0/) License, which permits use, distribution and reproduction in any medium, provided the original work is properly cited.

© 2024 The Author(s). *Studies in Applied Mathematics* published by Wiley Periodicals LLC.

to be non-zero when $c = 0$. In particular, we will study the equation

$$c_t = [(\nu + c)c_x]_x, \quad (2)$$

subject to the initial release of a finite quantity at $x = 0$, represented as a delta function. The dimensionless parameter ν will be assumed to be small. We thus suppose that

$$c \rightarrow 0 \text{ as } x \rightarrow \pm\infty, \quad c = 2\delta(x) \text{ at } t = 0. \quad (3)$$

This choice is not very restrictive, since when $\nu = 0$, any initial localized profile will tend to the similarity solution of (1) (which satisfies (3)) as t increases.

In fact, (2) may be a suitable modification of the porous medium equation to take into account the fact that the boundary condition in the far field is not that $c = 0$. For example, in the spread of a compressible fluid of (dimensionless) density ρ in a porous medium, an appropriate far field boundary condition for its governing porous medium equation would be $\rho = \nu$, corresponding to far field atmospheric air density. Putting $\rho = c + \nu$ regains (2) (with the boundary condition $c = 0$).

However, our principal motivation for this study lies in the motion of turbulent jets and plumes, in which a turbulent fluid flows into a quiescent ambient fluid. The plume is distinguished from the jet by the fact that its motion is partly or largely driven by its own buoyancy; the motion of a jet is due to its initial momentum. Theories for such motions have been pursued for almost a century.

Plumes occur ubiquitously in nature. Examples include volcanic eruptions, submarine black smokers, or simply smoke rising from a chimney. An example of a laboratory plume is shown in Figure 1. The equations governing the spread of a turbulent plume are outlined in the work of Garvey and Fowler.⁴ The mathematical theory to describe plumes was first proposed by Schmidt^{5,6} who provided a set of partial differential equations representing conservation of mass, momentum, and buoyancy. He used the lubrication approximation, in which the plume is considered to be narrow, and also the Boussinesq approximation, in which the variability of the density is only taken into account in the momentum equation. The buoyancy equation refers to conservation of the quantity that causes the density variation; for a thermal plume, this would be the temperature, and the buoyancy equation would be the energy equation, for example.

Schmidt used an eddy viscosity representation to describe the turbulence of the plume, with the eddy viscosity being described using Prandtl's mixing length theory. Schmidt took the mixing length to be the plume width. Experimental results indicate that the average plume structure is self-similar: for a cylindrical plume, the variables depend on r/z , where r is radial distance from the plume axis, and z is height above the source. It is also found that the radial profiles of vertical velocity and buoyancy are well represented by Gaussians (e. g., Ref. 7). Schmidt solved the similarity form of his equations (which are thus reduced to a set of ordinary differential equations) using the method of Frobenius, and found good agreement with his experimental results. It should be noted that Schmidt's use of an eddy viscosity gives the model a diffusive character (z playing the rôle of time) in which the solution domain is implicitly infinite in the radial direction, with boundary conditions (of zero velocity and buoyancy) being applied at $r = \infty$.

A different approach was initiated by Taylor,¹⁰ and pursued by Batchelor⁸ and Morton et al.⁹ This last paper has perhaps become the central pillar of subsequent theoretical developments. In this approach, the plume is taken to be of finite width, but the use of an eddy viscosity is eschewed. Instead, the Reynolds-averaged conservation laws are cross-sectionally integrated, using Taylor's¹⁰ proposed condition for entrainment at the plume edge. This provides a set of ordinary differen-



FIGURE 1 A laboratory plume. Photograph courtesy of Andy Woods.

tial equations for the moments of the variables. Closure of the equations can be achieved if the shapes of the cross-sectional profiles of the variables are assumed, and Fox¹¹ showed that Taylor's entrainment condition could then be deduced from the integrated conservation laws. It should be noted that if the plume is of finite width, then the derivation of the cross-sectionally averaged equations requires the Reynolds stress terms to vanish at the plume edge; this is in distinction to Schmidt's assumption.

These differing approaches raise the issue of whether a theoretical model of a plume should consider it to have finite or infinite width. In practice, this may seem to make little difference, because Gaussians decay so rapidly, but it does make a difference to the mathematical formulation of the problem, since the finite width plume theory of Morton et al.⁹ requires an entrainment condition to be prescribed, whereas the infinite plume theory does not.

Garvey and Fowler⁴ considered this issue from a theoretical viewpoint. If we presume that an eddy viscosity ν_T is appropriate, then if ν_T remains positive, the plume formally extends to infinity. The problem with this is that far from the plume, the ambient fluid will have a molecular viscosity ν_L ; this will be much less than the turbulent value, and this variation of viscosity

precludes the existence of a similarity solution, despite extensive experimental evidence that plumes are indeed self-similar.

Alternatively, we might suppose that the eddy viscosity vanishes when the vertical velocity w vanishes; it then turns out that because of the resulting degenerate diffusion (the eddy viscosity vanishes at the plume edge), the plume has finite width, but in addition, the entrainment condition is a consequence of the model, rather than having to be prescribed. The problem with this is that the resulting velocity profile reaches zero at the plume edge, and does not display the Gaussian tail.

Our hypothesis to reconcile these discrepancies is to suppose that a more realistic choice of viscosity is to take it to be $\nu_L + \nu_T$, where ν_T is generally much larger than the molecular value, but vanishes when $w = 0$. It is this choice which motivates our study of the simpler problem (2), representing as it does the same diffusive structure of the plume model, and in which the diffusivity combines the small “laminar” value ν and the larger “turbulent” value c . With ν being small, we expect that the similarity solution of the unperturbed ($\nu = 0$) model will remain approximately valid, but the non-zero value of ν enables the existence of a decaying tail. The present paper aims to validate this description as a proof of concept, which may then be applied to the more complex plume model.

2 | THE METHOD OF STRAINED COORDINATES

Our aim is to provide an asymptotic approximation to the solution of (2) when ν is small, in the form of a perturbation to the similarity solution, which can be written as

$$c = \begin{cases} \frac{3}{2x_f} \left[1 - \frac{x^2}{x_f^2} \right], & x < x_f, \\ 0, & x > x_f, \end{cases} \quad (4)$$

where the moving front is given by

$$x_f = 3^{2/3} t^{1/3} \quad (5)$$

e. g., Refs. 1, 12. On the face of it, this provides two parts of an outer solution that can be smoothly joined by a boundary layer at $x = x_f$. Specifically, if we put

$$x = x_f + \nu X, \quad c = \nu C, \quad (6)$$

then the leading order solution for C is found to be

$$C + \ln C = -\dot{x}_f X, \quad (7)$$

which satisfies

$$C \sim -\dot{x}_f X - \ln(-X) \text{ as } X \rightarrow -\infty. \quad (8)$$

The linear term matches to the similarity solution, but the logarithmic term must match to the second-order term in $x < x_f$.

This makes it awkward to provide a uniform approximation, and our purpose is to show that the use of the method of strained coordinates allows a uniform approximation to be obtained, without the necessity to consider separate approximations in regions close to and far from the front. This method is suggested for two reasons: the singularity of the unperturbed solution at $x = x_f$ is in reality shifted to $x = \infty$, and the higher order terms in the perturbation expansion become more singular at $x = x_f$; these are both features that suggest the method of strained coordinates.

Many of the details of the calculations of the present section are contained in the thesis of Garvey:¹³ see Section 3.2 on pages 69–76. The similarity solution (4) with (5) motivates a change of variables

$$\eta = \frac{x}{3^{2/3}t^{1/3}}, \quad c = \frac{1}{3^{2/3}t^{1/3}}f(\eta, \tau), \quad \tau = \ln t, \quad \varepsilon = 3^{2/3}\nu, \tag{9}$$

whence f satisfies

$$f_\tau = \frac{1}{3}(\eta f)_\eta + \frac{1}{9} \left[\left(\frac{1}{3}\varepsilon e^{\frac{1}{3}\tau} + f \right) f_\eta \right]_\eta; \tag{10}$$

importantly, f is symmetric in η , and

$$f \rightarrow 0 \text{ as } \eta \rightarrow \pm\infty, \quad \int_0^\infty f \, d\eta = 1. \tag{11}$$

The similarity solution when $\varepsilon = 0$ is

$$f_0 = \frac{3}{2}(1 - \eta^2) \tag{12}$$

for $\eta < 1$, and $f_0 = 0$ for $\eta > 1$.

For small positive ε , and assuming $t \ll \varepsilon^{-3}$, we adopt the method of strained coordinates (Refs. 14, 15) by writing

$$\begin{aligned} \eta &= s + \varepsilon\eta_1(s, \tau) + \varepsilon^2\eta_2(s, \tau) \dots, \\ f &= f_0(s) + \varepsilon f_1(s, \tau) + \varepsilon^2 f_2(s, \tau) \dots, \end{aligned} \tag{13}$$

and on expanding, we find that, if we define

$$\phi = f_1 + 3s\eta_1, \tag{14}$$

then ϕ satisfies

$$\phi_\tau = -\frac{1}{3}e^{\frac{1}{3}\tau} + \frac{1}{3} \left[\frac{1}{2}(1 - s^2)\phi_s \right]_s. \tag{15}$$

In view of the evenness of f , we have that η_1 is odd and f_1 is even; therefore, also ϕ is even.

The constraint on f_1 is that it should be no more singular than f_0 at $s = 1$ (Ref. 15), and, in fact, we can choose it to satisfy

$$f_1 = 0 \text{ at } s = 1, \quad (16)$$

and the integral constraint in (11) then leads to

$$\int_0^1 \phi \, ds = 0. \quad (17)$$

It is only the particular solution of (15) that is relevant, and this is

$$\phi = e^{\frac{1}{3}\tau} [\Phi(s) - 1], \quad (18)$$

where Φ satisfies Legendre's equation

$$[(1 - s^2)\Phi']' - 2\Phi = 0, \quad (19)$$

subject to Φ being even, and

$$\int_0^1 \Phi \, ds = 1. \quad (20)$$

One solution of (19) is the hypergeometric function

$$F\left[a, b, 1, \frac{(1-s)}{2}\right], \quad a + b = 1, \quad ab = 2, \quad (21)$$

and denoting this as $P(s)$, we can determine

$$P(s) = \sum_0^{\infty} p_n (1-s)^n, \quad p_n = \frac{\prod_0^{n-1} (r^2 + r + 2)}{2^n n!^2}, \quad (22)$$

with $p_0 = 1$. This function is analytic in $-1 < s < 3$, with a logarithmic singularity at $s = -1$. An even solution is then $P(s) + P(-s)$, but this is of no use, since we need the local behavior near $s = 1$, for which (22) does not help (for $P(-s)$). Frobenius's method gives an independent solution of the form

$$P(s) \ln\left(\frac{1-s}{2}\right) - G(s), \quad G = \sum_1^{\infty} p_n h_n (1-s)^n, \quad h_n = \sum_0^{n-1} \left\{ \frac{2}{r+1} - \frac{2r+1}{r^2+r+2} \right\}; \quad (23)$$

the coefficients $p_0 = 1$, $p_1 = 1$, $p_2 = 0.5$, $p_3 = 0.22$, and p_n continues to decrease by a factor of slightly more than 2 as n increases. The coefficients $h_1 = 1.5$, $h_2 = 1.75$, $h_3 = h_4 = 1.79$, and thereafter h_n decreases very slowly to a limit of $h_{\infty} \approx 1.66$.

To select a linear combination which is even, we define

$$\Phi^* = G(s) - P(s) \left\{ \alpha + \ln \left(\frac{1-s}{2} \right) \right\}, \tag{24}$$

and we choose α so that $\Phi^{*'}(0) = 0$; this yields

$$\alpha = \frac{P'(0) \ln 2 + P(0) + G'(0)}{P'(0)} \approx 1.561, \tag{25}$$

and it follows that

$$\Phi = \frac{\Phi^*(s)}{\int_0^1 \Phi^*(s) ds}, \tag{26}$$

where the normalizing factor is chosen to satisfy (20). From (19), we see that $\int_0^1 \Phi^*(s) ds = \lim_{s \rightarrow 1} \{(1-s)\Phi^{*'}\}$, and thus, from (24), $\int_0^1 \Phi^*(s) ds = 1$, so that $\Phi(s) = \Phi^*(s)$.

Returning whence we came, we have

$$f_1 + 3s\eta_1 = t^{1/3} \left[G(s) - 1 - P(s) \left\{ \alpha + \ln \left(\frac{1-s}{2} \right) \right\} \right]. \tag{27}$$

If there is no straining ($\eta_1 = 0$), then f_1 is singular at $s = 1$ (and thus also at $s = -1$), and the purpose of the straining is to remove the singularity. There is no unique way to do so, as is normal in this procedure. In view of (16), we require

$$\eta_1 \sim \frac{1}{3} t^{1/3} \left[\ln \left(\frac{2}{1-s} \right) - (1 + \alpha) \right] \text{ as } s \rightarrow 1; \tag{28}$$

a simple choice of an odd η_1 is to take

$$\eta_1 = \frac{1}{3} t^{1/3} \left[\ln \left(\frac{1+s}{1-s} \right) - (1 + \alpha)s \right], \tag{29}$$

and consequently,

$$f_1 = t^{1/3} \left[G(s) - 1 - P(s) \left\{ \alpha + \ln \left(\frac{1-s}{2} \right) \right\} - s \ln \left(\frac{1+s}{1-s} \right) + (1 + \alpha)s^2 \right]. \tag{30}$$

Equations (29) and (30), together with (13), provide an approximate solution of the perturbed model. In view of (29), we see that as $s \rightarrow 1$ and thus $f \rightarrow 0$, $\eta \rightarrow \infty$, providing a decaying tail to the distribution. However, the tail is not Gaussian, but exponential. In detail, we have, as $s \rightarrow 1$,

$$f \sim 0.463 \exp \left[\frac{3(1-\eta)}{\varepsilon t^{1/3}} \right] \text{ for } \eta \gtrsim 1, \tag{31}$$

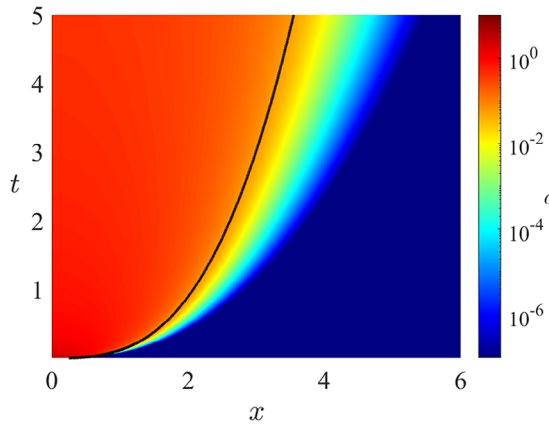


FIGURE 2 Method of lines solution of (2) showing $c(x, t)$ as a colored contour plot using a value $\varepsilon = 0.1$ (or equivalently $\nu \approx 0.0481$). The black line gives the front position when $\varepsilon = 0$.

where the prefactor is $6 e^{-(1+\alpha)}$. (We use the symbol ‘ \gtrsim ’ to denote “greater than or of the same order as.”) Our overall solution is given by

$$\eta = s + \frac{1}{3}\varepsilon t^{1/3} \left[\ln \left(\frac{1+s}{1-s} \right) - (1+\alpha)s \right],$$

$$f = \frac{3}{2}(1-s^2) + \varepsilon t^{1/3} \left[G(s) - 1 - P(s) \left\{ \alpha + \ln \left(\frac{1-s}{2} \right) \right\} - s \ln \left(\frac{1+s}{1-s} \right) + (1+\alpha)s^2 \right]. \quad (32)$$

3 | NUMERICAL RESULTS

We have solved the partial differential equation (2) numerically using the method of lines, and here we compare the results to the approximate solution (32). The initial condition is taken to be a Gaussian approximation of the Dirac delta function,

$$c(x, 0) = \frac{1}{\sqrt{2\pi\varepsilon_L}} \exp \left(-\frac{x^2}{2\varepsilon_L} \right), \quad (33)$$

and we use a value $\varepsilon_L = 0.0005$. The infinite spatial domain is replaced by $[-x_m, x_m]$, so that the numerical boundary conditions are taken as

$$c = 0 \text{ on } x = \pm x_m. \quad (34)$$

The value of x_m used in the calculations is $x_m = 10$.

First, Figure 2 shows the numerical solution of (2) as a color map. This figure highlights how the inclusion of ν affects the solution of the nonlinear diffusion equation. If $\nu = 0$, the similarity solution would have a sharp boundary (indicated by the black line), but with $\nu > 0$, it can be seen that the front is spread out.

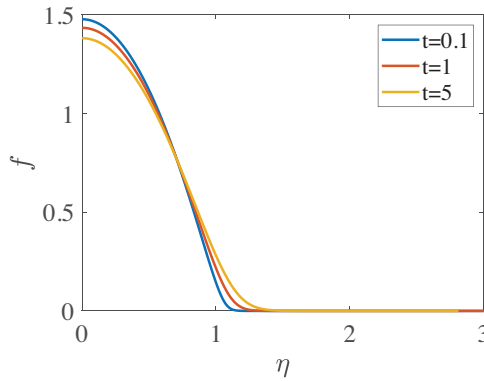


FIGURE 3 Method of lines solution of (2) for $\nu = 0.1$. The value of $\varepsilon = 3^{2/3}\nu \approx 0.208$.

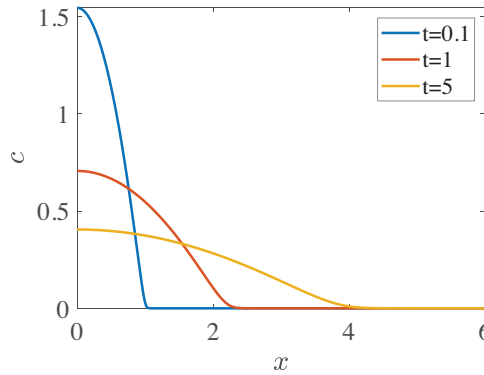


FIGURE 4 The same three plots of the numerical solution as in Figure 3, but returned to the original variables c and x .

Next, we show in Figure 3 the effect of $\nu > 0$ on the similarity solution. If $\nu = 0$, then $f \rightarrow 0$ as $\eta \rightarrow 1$ independently of t . For $\nu > 0$, the solution spreads slowly in similarity space, and acquires an exponentially decaying tail. The same sequence of plots is shown in Figure 4, but now plotting c as a function of x at different times. The corresponding asymptotic approximate solutions are not shown, as they are not readily distinguishable.

A comparison of the numerical and asymptotic solutions for a value of $\varepsilon = 0.1$ is given in Figure 5, which shows $\ln c$ versus x for different times. The dashed lines represent the asymptotic approximation in (32), while the full lines give the numerical solution. The log-linear plot allows the discrepancies between the numerical and asymptotic solutions to be illustrated. At small times, the approximate solution is uniformly good, but it deviates from the exponential tail at larger times. The numerical solution appears at first sight to retain its exponential tail, but its slope departs increasingly from that of the asymptotic solution.

What is surprising about this is not so much that it occurs, but that the departure is so rapid. Since the small parameter in the expansion is $\delta = \varepsilon t^{1/3}$ in (32), this increases as t increases. For the three graphs from left to right in Figure 5, the values of δ are 0.05, 0.1, and 0.17, and we might expect the approximation to worsen, as indeed it does.

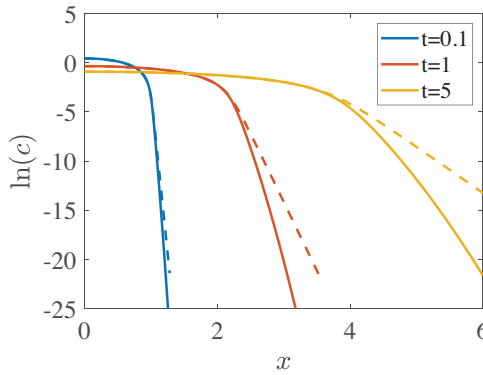


FIGURE 5 Numerical (full lines) and asymptotic (dashed lines, (32)) solutions of (2) in a log-linear plot of $\ln c$ against x at different times using the value $\nu = 0.0481$ (so $\varepsilon = 0.1$).

In fact, the basis for the approximation breaks down when $c \ll \nu$. This is most easily seen in consideration of (2), where the basis for the approximation requires $c \gg \nu$. The transition to the exponential tail is given by (7), for example, and this shows that as x increases beyond the front position, the exponential tail satisfies

$$c \sim \nu \exp \left[-\frac{\dot{x}_f(x - x_f)}{\nu} \right], \tag{35}$$

and for $x > x_f$, this motivates the definition

$$c = \nu \exp \left[\frac{\psi}{\nu} \right], \tag{36}$$

whence (2) becomes approximately (ignoring the exponentially small $c \ll \nu$)

$$\psi_t = \psi_x^2 + \nu \psi_{xx}, \tag{37}$$

and (35) requires

$$\psi \sim -\dot{x}_f(x - x_f) \text{ as } x \rightarrow x_f. \tag{38}$$

The condition that $c \rightarrow 0$ as $x \rightarrow \infty$ requires $\psi \rightarrow -\infty$ there.

Equation (37) and its matching condition (38) provide a suitable approximation of the model when $x - x_f$ is positive and $O(1)$. Equation (37) is just an integrated form of Burgers' equation, which is unsurprising since (36) is an inverse Hopf–Cole transformation. Note also that (36) is really a WKB approximation to (2).

At leading order, $\psi_t = \psi_x^2$, and the solution of this satisfying (38) can be obtained using Charpit's method, and is given parametrically by

$$\begin{aligned} \psi &= -(t - \tau)\dot{x}_f^2, \\ x &= x_f + 2(t - \tau)\dot{x}_f, \end{aligned} \tag{39}$$

where

$$x_f = 3^{2/3}\tau^{1/3}, \quad \dot{x}_f = \frac{1}{3^{1/3}\tau^{2/3}}, \quad (40)$$

and from this, we find

$$\psi_x = -\dot{x}_f. \quad (41)$$

The second equation in (39) provides an implicit definition of $\tau(x, t)$, and consideration of the graph of x versus τ shows that for each value of t , τ is a monotonically decreasing function of x , with $\tau = t$ at $x = x_f$, and $\tau \rightarrow 0$ as $x \rightarrow \infty$, and specifically

$$\tau^{2/3} \sim \frac{2t}{3^{1/3}x} \text{ as } x \rightarrow \infty, \quad (42)$$

and thus,

$$\psi \sim -\frac{x^2}{4t} \text{ as } x \rightarrow \infty. \quad (43)$$

We see from this that the exponential “tail” is not the real tail at all, and beyond the front, the decaying tail is, in fact, a Gaussian (as indeed one should expect). This explains the deviation of the asymptotic solution from the numerical solution in Figure 5, but whether it matters is a moot point, since it is only evident when c is exponentially small. The figure accentuates the discrepancy, but it is not visible on a linear–linear plot.

4 | CONCLUSIONS

In this work, we have shown how the method of strained coordinates can be used to obtain satisfactory approximate solutions to a weakly perturbed degenerate nonlinear diffusion equation, which serves as a prototype groundwater flow problem, but also as a toy representation of mixed laminar-turbulent flows, such as occur in jets and plumes. It provides a useful example of this method, which is not one that is commonly used, and it also provides a potential vehicle for the comparable description of buoyant plumes.

ACKNOWLEDGMENTS

A. C. F. acknowledges the support of the Mathematics Applications Consortium for Science and Industry (www.macsi.ul.ie) funded by the Science Foundation Ireland mathematics grant 12/IA/1683. This publication has emanated from research conducted with the financial support of Science Foundation Ireland under Grant number 18/CRT/6049. For the purpose of Open Access, the author has applied a CC BY public copyright licence to any Author Accepted Manuscript version arising from this submission.

Open access funding provided by IReL.

DATA AVAILABILITY STATEMENT

Data sharing not applicable to this article as no datasets were generated or analyzed during the current study.

ORCID

R. S. Garvey  <https://orcid.org/0000-0002-0797-0056>

REFERENCES

1. Ockendon J, Howison S, Lacey A, Movchan A. *Applied Partial Differential Equations: Revised Edition*. Oxford University Press; 2003.
2. Vazquez JL. *The Porous Medium Equation: Mathematical Theory*. Oxford University Press; 2006.
3. Witelski TP, Bernoff AJ. Self-similar asymptotics for linear and nonlinear diffusion equations. *Stud Appl Math*. 1998;100:153-193.
4. Garvey RS, Fowler AC. On the mathematical theory of plumes. *Geophys Astrophys Fluid Dyn*. 2023;117(2):79-106.
5. Schmidt W. Turbulente Ausbreitung eines Stromes erhitzter Luft. I. Teil. *Z angew Math Mech*. 1941;21(5):265-278.
6. Schmidt W. Turbulente Ausbreitung eines Stromes erhitzter Luft. II. Teil. *Z angew Math Mech*. 1941;21(6):351-363.
7. Rouse H, Yih CS, Humphreys HW. Gravitational convection from a boundary source. *Tellus*. 1952;4(3):201-210.
8. Batchelor GK. Heat convection and buoyancy effects in fluids. *Quart J Roy Meteorol Soc*. 1954;80(345):339-358.
9. Morton BR, Taylor G, Turner JS. Turbulent gravitational convection from maintained and instantaneous sources. *Proc R Soc Lond A*. 1956;234(1196):1-23.
10. Taylor GI. Dynamics of a mass of hot gas rising in air. U. S. Atomic Energy Commission MDDC 919. LADC 276. 1945. [*The reference is that given by Morton et al.(1956). The report itself only refers to 'LA report 236'.*].
11. Fox DG. Forced plume in a stratified fluid. *J Geophys Res*. 1970;75(33):6818-6835.
12. King JR. Exact similarity solutions to some nonlinear diffusion equations. *J Phys A: Math Gen*. 1990;23(16):3681-3697.
13. Garvey RS. *Aspects of Mass Extinctions*. Ph.D. thesis. University of Limerick; 2024. Available at doi:10.34961/researchrepository-ul.26146924.v1
14. Lighthill MJ. A technique for rendering approximate solutions to physical problems uniformly valid. *Phil Mag (VII)*. 1949;40:1179-1201.
15. Van Dyke MD. *Perturbation Methods in Fluid Mechanics*. Parabolic Press; 1975.

How to cite this article: Garvey RS, Fowler AC. Weak long-range diffusion. *Stud Appl Math*. 2024;e12759. <https://doi.org/10.1111/sapm.12759>